

Article

# System Reliability Assessment of Cable-Supported Bridges under Stochastic Traffic Loads Based on Deep Belief Networks

Naiwei Lu <sup>1,2,\*</sup> , Yang Liu <sup>2,3</sup>, Mohammad Noori <sup>4</sup>  and Xinhui Xiao <sup>3</sup>

<sup>1</sup> Industry Key Laboratory of Traffic Infrastructure Security Risk Management, Changsha University of Science and Technology, Changsha 410114, China

<sup>2</sup> School of Civil Engineering, Changsha University of Science and Technology, Changsha 410114, China; ly@hut.edu.cn

<sup>3</sup> School of Civil Engineering, Hunan University of Technology, Zhuzhou 412007, China; xiaoxinhui@hut.edu.cn

<sup>4</sup> Department of Mechanical Engineering, California Polytechnic State University, San Luis Obispo, CA 93407, USA; mnoori@calpoly.edu

\* Correspondence: lunaiwei@csust.edu.cn; Tel.: +86-137-8726-5433

Received: 12 October 2020; Accepted: 9 November 2020; Published: 13 November 2020



**Abstract:** A cable-supported bridge is usually a key junction of a highway or a railway that demands a higher safety margin, especially when it is subjected to harsh environmental and complex loading conditions. In comparison to short-span girder bridges, long-span flexible structures have unique characteristics that increase the complexity of the structural mechanical behavior. Therefore, the system safety of cable-supported bridges is critical but difficult to evaluate. This study proposes a novel and intelligent approach for system reliability evaluation of cable-supported bridges under stochastic traffic load by utilizing deep belief networks (DBNs). The related mathematical models were derived taking into consideration the structural nonlinearities and high-order statically indeterminate characteristics. A computational framework is presented to illustrate the steps followed for system reliability evaluation using DBNs. In a case study, a prototype suspension bridge is selected to investigate the system reliability under stochastic traffic loading based on site-specific traffic monitoring data. The numerical results indicated that DBNs provide an accurate approximation for the mechanical behavior accounting for structural nonlinearities and different system behaviors, which can be treated as a meta-model to estimate the structural failure probability. The dominant failure modes of the suspension bridge are the fracture of suspenders followed by the bending failure of girders. The degradation of suspenders due to fatigue-corrosion damage has a significant effect on the system reliability of a suspension bridge. The numerical results provide a theoretical basis for the design on cable replacement strategies.

**Keywords:** system reliability; deep belief network; cable-supported bridge; fault tree; stochastic traffic flow; fatigue-corrosion damage

## 1. Introduction

The current transportation market, driven by a steady increase in global, is growing rapidly driven by a steady increase in the global economy, especially in developing countries [1]. There is an urgent demand for constructing highways and railways in mountainous and cross-sea areas, where long-span bridges are widely built or in construction [2]. Cable-supported bridges, including cable-stayed bridges and suspension bridges, are widely used in highways crossing gorges, rivers, and gulfs, due to their superior structural mechanical property and beautiful appearance [3]. A cable-supported

bridge is usually the key junction of a highway or a railway demanding a higher safety margin. However, long-span bridges suffer from harsh environmental effects and complex loading conditions, such as heavy traffic loading, significant wind load effects, severe corrosion effects, and other natural disasters [4–6]. Subsequently, these effects may result in changes in the structural-mechanical behavior, which may alter the dynamic characteristics and resistance of the bridge during its lifetime. Due to the structural flexibility of cable-supported bridges, wind load and seismic effect are critical factors affecting bridge safety [7,8]. Furthermore, the steadily growing traffic load and environmental corrosion effects can lead to bridge safety degradation [9,10]. Therefore, it's critical to ensure the structural safety of cable-supported bridges in harsh environments.

Cable-supported bridges have one or more pylons and flexible decks supported by prestressed cables. The cables are critical components to support girder gravity and moving vehicle loads [11]. However, cables are subjected to corrosion under the coupling effect of fatigue loading and environmental corrosion. As a result, cable corrosion can lead to strength degradation, which can result in cable rupture or even collapse of the bridge. A research conducted by Mehrabi et al. [12] revealed that more than half of the stay cables of an in-service cable-stayed bridge were severely corroded, demanding prompt replacement. Cable-supported bridges are associated with numerous uncertainties, such as material performance behaviors, cross-sectional dimensions, and various external loads. These uncertainties make the safety analysis of cable-supported bridges more complex for two main reasons. First, the structural mechanical behavior is highly nonlinear. Second, the bridge structure is statically indeterminate, which may lead to a failure sequence of more complicated systems.

System reliability theory is a powerful tool for the estimation of the life-cycle safety of cable-supported bridges accounting for uncertainties [13,14]. For a statically indeterminate structure, the scenario of a component failure may not result in safety issues. For example, the rupture of a stay cable may not affect the safety and serviceability of a cable-stayed bridge. However, a progressive failure of critical components may result in safety problems or even a bridge collapse event. The system reliability theory can be employed to search for potential failure sequences and identify sensitive components or parameters, which is beneficial for design optimization. There are two critical problems in structural system reliability evaluation. First and foremost, long-span bridges have a higher indeterminate degree that makes the structural performance functions more complicated. Thus, it is important to accurately and efficiently approximate the limit state function by utilizing an adequate approach. In this regard, there are several commonly used approaches, such as the artificial neural network (ANN) and the respond surface method (RSM). With the rapid development of artificial intelligence (AI), the application of AI-based approaches in structural reliability analysis is becoming increasingly popular. Dai et al. [15] proposed a least squares support vector regression (LS-SVR) for structural reliability analysis with high efficiency and accuracy. Lu et al. [16] utilized a machine learning approach to estimate the system reliability of a cable-stayed bridge considering cable damage due to fatigue and corrosion effects. Deep learning is a recently developed ANN approach that is widely used in the fields of graphics and image recognition [17]. A deep belief network (DBN) is a type of deep learning method that is commonly used for probability training [18]. DBN is feasible for approximating the structural mechanical behavior, which is the basis for subsequent reliability evaluation. Compared to traditional AI-based approaches, DBN has the following advantages [19–21]. First, it utilizes hidden layers which are more efficient compared to traditional multilayer perceptions, such as the back-propagation (BP) neural networks, and thus the training process is time-saving. Second, DBN has a deep architecture like a mammal brain, which is able to capture the depth nonlinearity of a structural complex system, while SVM is a shallow architecture benefiting from the nonlinear kernel function. Finally, DBN is more robust in the classification of various data with large-scale parameters.

The second critical problem is how to search for the failure sequence of a system efficiently. In this regard, the most commonly used approach is the  $\beta$ -bound approach that utilizes the reliability index range to determine the components that are likely to fail. Li and Song [22] presented a branch-and-bound method together with the finite element (FE) method to update the limit state

function. Kang et al. [23] developed a matrix-based system reliability method to replace the failure tree of complex structures. Liu et al. [24] proposed an adaptive SVR approach combined with the advanced  $\beta$ -bound approach to develop the fault tree of a pre-stressed concrete cable-stayed bridge.

This study proposes a novel and intelligent approach for system reliability evaluation of cable-supported bridges under stochastic traffic load by utilizing DBNs. Mathematical models for the system reliability of cable-supported bridges were derived taking into consideration structural nonlinearities and high-order statically indeterminate characteristics. A computational framework was developed to exhibit the procedures for system reliability evaluation using DBNs. In a case study, a prototype suspension bridge was selected to investigate the system reliability under stochastic traffic loading considering site-specific traffic monitoring data. Numerical results indicated the feasibility of utilizing DBN as a meta-model to estimate the structural failure probability. The dominant failure mode of the suspension bridge was determined, and the effect of cable degradation due to fatigue-corrosion damage on the system reliability of the suspension bridge was investigated.

## 2. Mathematical Model for Bridge System Reliability

### 2.1. Nonlinear Limit State Functions

A cable-supported bridge has long-span flexible girders that increase the complexity of the structural mechanical behavior. In general, a cable-supported bridge has numerous failure modes. The critical failure modes are the bending moment failure of stiffening girders and cable rupture. The serviceability failure of a structural system derives from large deflections and severe vibrations. In this regard, the performance functions of the failure modes can be written as:

$$Z_i = 1 - \frac{P^i(\mathbf{X})}{P_u^i} - \frac{M^i(\mathbf{X})}{M_u^i} \quad (i = 1, \dots, m) \quad (1)$$

$$Z_j = T_u^j - T^j(\mathbf{X}) \quad (j = 1, \dots, n) \quad (2)$$

$$Z_u = u_{\max} - u(\mathbf{X}) \quad (3)$$

where  $\mathbf{X}$  denotes the random variables;  $m$  and  $n$  are respectively the number of girders and cables that are likely to fail;  $P_u^i$  and  $M_u^i$  are the ultimate axial force and ultimate bending moment for the  $i$ th element, respectively;  $P^i(\mathbf{X})$  and  $M^i(\mathbf{X})$  are respectively the actual axial forces and bending moments of the  $i$ th element;  $u_{\max}$  is the threshold load effect associated with bridge serviceability; and  $T_u^j$  and  $T^j(\mathbf{X})$  are the cable tensional strength and the actual cable force, respectively. For the threshold deflection of bridge girders,  $u_{\max} = L_b/500$ , where  $L_b$  is the span length of the bridge. It should be noted that the limit state functions are nonlinear and implicit, which can be approximated by the following DBNs.

### 2.2. Cable Strength Degradation Modeling

It is known that the cables in a cable-supported bridge are prone to damage due to corrosion and fatigue. The average service time of a bridge cable is usually 20 years. Thus, in the reliability and safety evaluation, cable strength degradation should be taken into consideration. In general, cable damage can be considered in a parallel-series model accounting for the effect of cable length and number of cables [25]. In addition, in order to incorporate the cable strength degradation due to the fatigue-corrosion effect, cable strength can be derived from the strength of a wire using a modified Weibull distribution, which can be written as [26]:

$$F_Z(z) = 1 - \exp\left[-\lambda\left(\frac{z}{u}\right)^k\right] \quad (4)$$

where  $z$  is the strength of a short wire,  $u$  and  $k$  are the distribution parameters in a conventional Weibull function,  $\lambda = L/LL_0$  is a scale parameter representing the fatigue-corrosion effect,  $L_0$  is the length of a

wire specimen, and  $lL_0$  is the correlation length of the wire. A higher  $\lambda$  indicates a severer damage to the cable and a smaller correlation length.

To model the probability distribution of a parallel-series system, a cable consisted of  $n$  wires was considered. Faber et al. [27] provided the probability distribution of a cable based on the aforementioned Weibull distribution. The mean and standard deviation are:

$$E(n) = nx_0(1 - F_Z(x_0)) + c_n \tag{5}$$

$$D(n) = x_0[nF_Z(x_0)(1 - F_Z(x_0))]^{1/2}, \tag{6}$$

where  $c_n = 0.966an^{1/3}$ ,  $a^3 = \frac{f_Z^2(x_0)x_0^4}{(2f_Z(x_0)+x_0f'(x_0))}$ ,  $x_0 = \left[\frac{L_0}{Lk}\right]^{1/k} \sigma_u$ ,  $\sigma_u$  is the ultimate stress of a wire, and  $f_Z(x_0)$  is a probability density function following Weibull distribution.

To model the cable strength degradation model, an experimental study on the strength of corroded cables with a service time of 20 years was considered [28]. Figure 1 presents the probability density function (PDF) of the cable strength of three types of short wires, including a new wire, an uncorroded wire, and a corroded wire. It can be observed that the mean strength value of the corroded wire was the lowest. In addition, the shape of the distribution changed significantly due to the corrosion-fatigue effect.

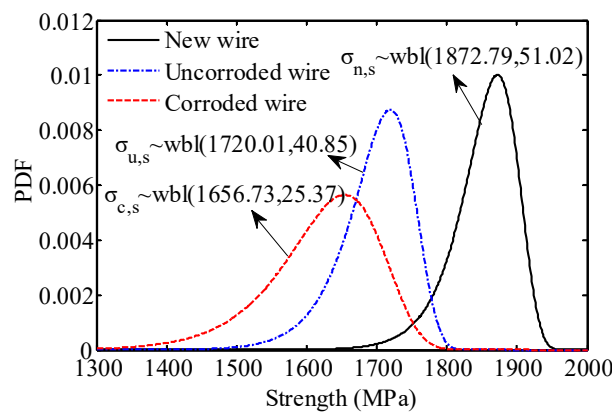


**Figure 1.** Comparison of the PDFs of the short wire strength accounting for fatigue damage and corrosion.

According to the research conducted by Lu et al. [16], the degradation curves of a cable can be obtained by:

$$y_1(t) = -1.5 \times 10^{-5}t^2 - 3.2 \times 10^{-3}t + 0.998 \tag{7}$$

$$y_2(t) = -4.7 \times 10^{-4}t^2 - 2.4 \times 10^{-3}t + 0.996 \tag{8}$$

where  $t$  is the service time in years, and  $y_1$  and  $y_2$  are the degradation functions for the uncorroded and corroded cables, respectively. It can be concluded that the mean cable strength of the uncorroded and corroded cables decreased significantly during the service lifetime. In addition, the deviation of the probability was significantly affected by the corrosion effect.

The cable strength of a cable with a number of long wires is usually modeled as an equivalent normal distribution function using Equations (5) and (6), as suggested by Faber et al. [27]. Considering a cable with parallel steel wires of  $L_b = 232$  m,  $n = 243$ , and  $\sigma_u = 1766$  MPa, the equivalent normalized PDFs of the corroded, uncorroded and new cables are shown in Figure 2. It can be observed that the standard deviation exhibited a slight unexpected decrease. This phenomenon might due to the equivalent normalization in the series-parallel system of the cable.

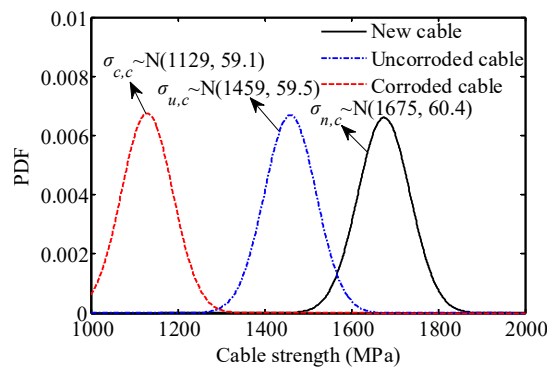


Figure 2. Comparison of the normalized PDFs of wire strength accounting for cable corrosion.

By combining the PDFs of different wires (as shown in Figure 1), the time-varying PDF of the cable strength can be estimated. Therefore, based on Figure 2 and Equations (7) and (8), the time-varying PDFs were obtained (as shown in Figure 3). As it can be observed in Figure 3, the probabilistic characteristics of the corroded and uncorroded cables were totally different. The corroded cable exhibited a severer downward tendency, while the uncorroded cable presented a slight downward tendency. This phenomenon demonstrates that corrosion is a critical factor that should be taken into account in probability modeling of the cable strength. Moreover, the degradation model can be utilized for the time-varying reliability analysis of a cable-supported bridge. The analytical results can be the theoretical basis for cable replacements.

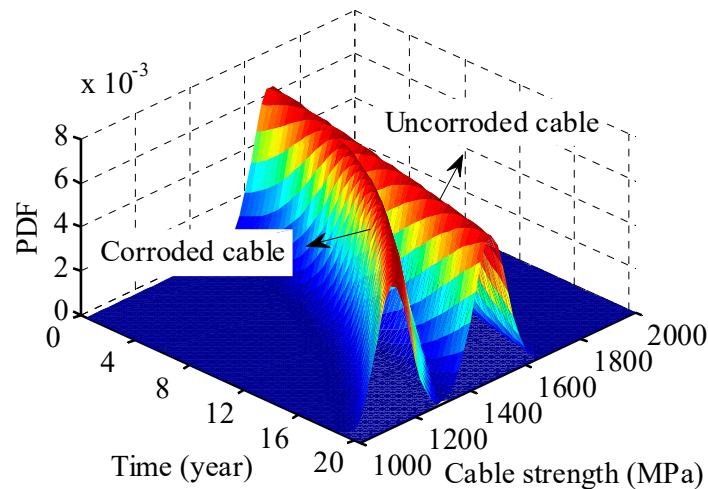


Figure 3. Degradation of the cable strength accounting for corrosion.

Additionally to the fatigue-corrosion effect, there are several factors that may lead to cable strength degradation, such as wind loads and seismic loads. Since, in the present study, the cable strength degradation model in the present study is derived based on a service time of 20 years, these environmental factors were comprehensively considered. The probability model of cable strength degradation was utilized for the time-varying reliability analysis of the suspension bridge.

### 2.3. System Failure Modeling

In general, the structural system of a cable-supported bridge can be simplified as several events  $E_s$ , which is made of individual failure event  $E_i$  ( $i = 1, \dots, m$ ). In general,  $E_i$  consists of several components  $E_i^j$  ( $j = 1, \dots, n$ ) in sequence. Based on the above assumption, the structural system can be modeled as:

$$\begin{cases} E_i = \bigcap_{j=1}^n E_i^j \\ E_s = \bigcup_{i=1}^m E_i \end{cases} \quad (9)$$

According to Equation (9), the system failure events are combined in parallel with several failure states, while a failure state is composed of several components in series. Therefore, the system failure of the bridge can be described as a series-parallel connection system. The critical step is to develop the fault tree of the bridge taking into consideration components that are likely to fail. As mentioned earlier, the most commonly used approach to search for components that are likely to fail in a structure is the  $\beta$ -bound method. The principle of the  $\beta$ -bound method will be illustrated below, and details of the approach can be found in Liu et al. [24].

Considering several components that are likely to fail in a system, the critical components should satisfy the reliability range according to the  $\beta$ -bound method:

$$\beta_{r_k}^{(k)} = [\beta_{\min}^{(k)}, \beta_{\min}^{(k)} + \Delta\beta^{(k)}] \quad (10)$$

where  $k$  represents the  $k$ -th stage of the failure process,  $\beta_{r_k}$  represents the conditional reliability index, and  $\beta_{\min}$  and  $\Delta\beta$  are the minimum reliability index and the step of reliability index range, respectively. It is recommended that  $\Delta\beta$  is 3 in the first stage, and 1 in the following stages.

Once the fault tree has been developed using the  $\beta$ -bound method, the narrow boundary of the structural system is considered, which can be written as:

$$P_{f_{ij}} = \max[P_A, P_B] + \min[P_A, P_B] \left( \frac{\pi - 2\arccos(\rho_{ij})}{\pi} \right) \quad (11)$$

$$\begin{cases} P_A = \Phi[-\beta_i] \Phi \left[ -\frac{\beta_i - \rho_{ij}\beta_j}{\sqrt{1-\rho_{ij}^2}} \right] \\ P_B = \Phi[-\beta_j] \Phi \left[ -\frac{\beta_j - \rho_{ij}\beta_i}{\sqrt{1-\rho_{ij}^2}} \right] \end{cases} \quad (12)$$

where  $\beta_i$  and  $\beta_j$  are the reliability indices of the  $i$ th and  $j$ th components, respectively,  $\rho_{ij}$  is the correlation coefficient of the  $i$ th and  $j$ th components, and  $\Phi()$  is the cumulative distribution function of the random variable following the standard normal distribution.

## 3. A reliability Evaluation Framework Based on DBNs

### 3.1. Theoretical Basis of DBNs

In general, a DBN is a new type of generative neural networks which are constructed by stacking restricted Boltzmann machines (RBMs) that are usually trained based on the probability principle [29]. In a DBN, the RBMs are connected between hidden and visible layers. In the visible layer, the nodes are connected without directions. In the pre-training stage, the main training strategy is unsupervised learning, where the fine-tuning stage is trained by a supervised learning method. The outputs of a visible layer are treated as inputs to the hidden layer. In general, DBNs are widely used in the field of image identification. Their application in structural reliability analysis is relatively insufficient. In this study, the DBN and BP networks were utilized to approximate the structural response surface

functions. The framework of predicting the effect of structural load effect using the DBN is shown in Figure 4. The DBN principle will be demonstrated below.

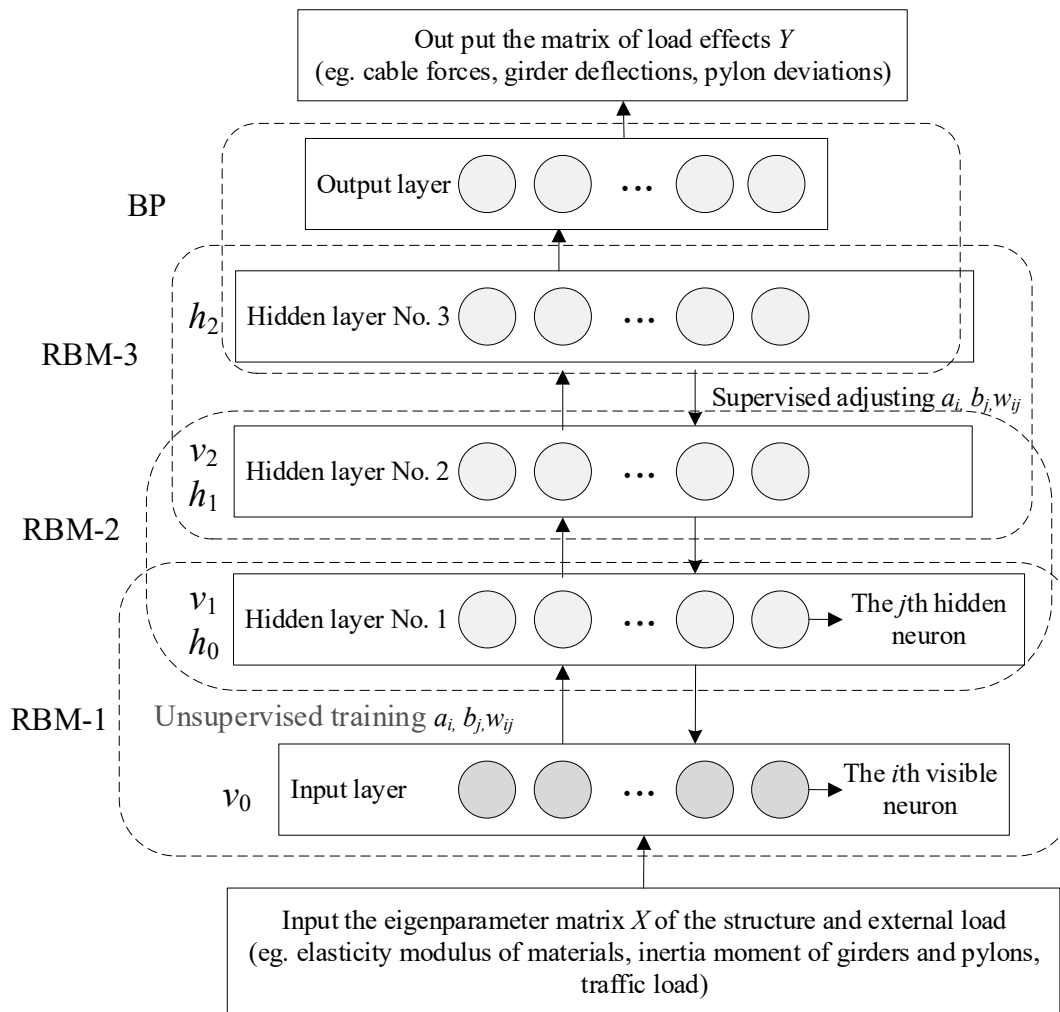


Figure 4. Flowchart of structural load effect prediction based on DBNs.

The energy function of a joint structure  $(V, H)$  of visible and hidden units can be written as:

$$E(V, H) = -\sum_{i=1}^m a_i v_i - \sum_{j=1}^n b_j h_j - \sum_{j=1}^n \sum_{i=1}^m v_i h_j w_{ij} \tag{13}$$

where  $V = (v_1, v_2, v_3, \dots, v_m)$  is a visible layer,  $H = (h_1, h_2, h_3, \dots, h_n)$  is a hidden layer,  $m$  and  $n$  are the number of element in the visible and the hidden layer, respectively;  $v_i$  and  $h_j$  are the  $i$ th and  $j$ th neurons in the visible and hidden layers, respectively;  $w = (w_{ij})$  is the weight of elements, and  $a_i$  and  $b_j$  are the bias in the visible layer and the hidden layer, respectively.

As it can be seen in Figure 4, the parameters  $a_i, b_i,$  and  $w_{ij}$  are trained and optimized from bottom to top based on an unsupervised learning method. Subsequently, the parameters are adjusted from top to bottom. The training function is:

$$w = w + \zeta \left[ P(h_j^{(k)} = 1 | v^{(k)}) (v^{(k)})^T - P(h_j^{(k+1)} = 1 | v^{(k+1)}) (v^{(k+1)})^T \right] \tag{14}$$

$$a = a + \zeta (v^{(k)} - v^{(k+1)}) \tag{15}$$

$$b = b + \zeta \left[ P(h_j^{(k)} = 1 | v^{(k)}) - P(h_j^{(k+1)} = 1 | v^{(k+1)}) \right] \tag{16}$$

where  $P$  is a probability function,  $\zeta$  is the training rate which is in the range of 0.05 and 0.2, and  $h_j^{(k)}$  is the  $k$ th optimization of the  $j$ th neuron in the hidden layer.

### 3.2. Proposed Computational Framework

In Figure 5, a computational framework is presented to illustrate the approach of utilizing the DBN to estimate the reliability of a cable-supported bridge. Detailed descriptions of the followed computational steps are summarized below.

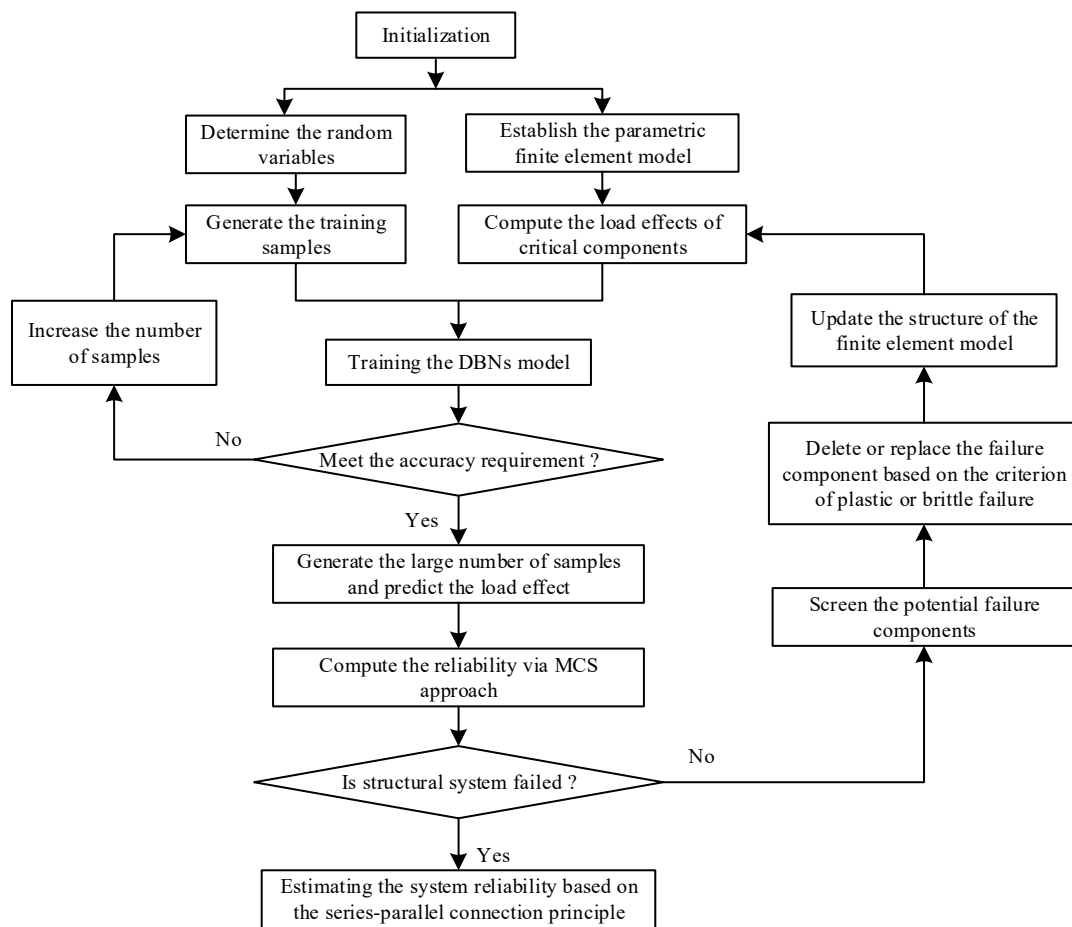


**Figure 5.** Flowchart of evaluating system reliability of a cable-stayed bridge via DBNs.

In the first step, the critical random variables, such as the cable and concrete elasticity modulus, and the cross-sectional inertia moments of girders and pylon elements, are selected. The training samples should be selected according to the probability distribution of these random variables, which will be used to train the mechanical behavior of the bridge structure.

In the second step, a parametric finite element model is developed using a commercial software, such as ANSYS or MIDAS. It is recommended to use ANSYS for the FE modeling, since its APDL code can be connected with MATLAB script files.

In the third step, the DBNs are trained the generated samples as the input data and the FE results as the output data. The number of hidden layers should be optimized based on the production accuracy of the DBNs. If the accuracy is not sufficient, the number of training samples will be increased. This will improve the prediction accuracy, but will increase the computational cost.

In the fourth step, a large number of samples are generated by using the Monte Carlo simulation (MCS) according to the probability distribution of the random variables. Subsequently, the load effect of the critical components is predicted taking into consideration the samples of the random variables. Therefore, structural reliability can be estimated by counting the number of failure samples.

In the fifth step, the load-carrying capability of the residual structure is checked with consideration of the potential failure of one of the critical components. The system failure criterion is defined as when the structural system has lost its load-carrying capacity, or when the structural deflection is so large enough that it cannot carry the external load. Such critical states are extremely dangerous for in-service bridges, since the bridge is possible to collapse at any time.

In the sixth step, the components that are likely to fail are deleted or replaced based on the criterion of plastic or brittle failure. For example, cable failure is brittle, and the corresponding updating approach is to delete the failed cables. On the other hand, the bending failure of a girder is plastic, and thus the corresponding updating approach is to add a plastic hinge at the failure point. Subsequently, the structural system is updated, and the process goes back to the second step.

Finally, based on the above steps, all failure sequences are screened out. The correlation coefficient matrix can be estimated for the system reliability evaluation, and the system event tree can be estimated considering the critical failure sequences. Eventually, the system reliability can be assessed based on the series-parallel connection criterion.

#### 4. Case Study of a Suspension Bridge

##### 4.1. Prototype Suspension Bridge Characteristics

The prototype bridge used in the present study is the Nanxi Yangtze River Bridge, which is a suspension bridge in the Luyu highway of China. The general arrangement and the serial number of each component are shown in Figure 6. The main cable is composed of parallel wire strands, the stiffening girders are steel box girders, and the pylon has a concrete box section. According to the construction sequence, the suspenders, main cables, and girders are divided into 64 segments. Details of the bridge characteristics can be found in Lu et al. [1].

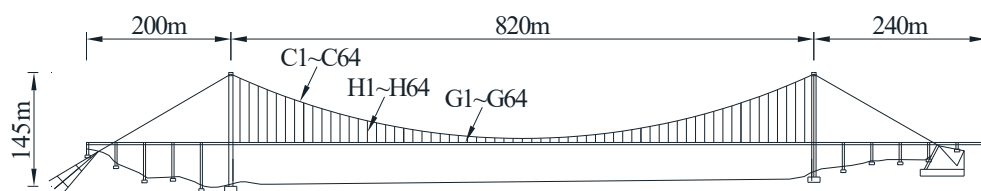


**Figure 6.** General arrangement and serial number of components of the Nanxi Yangtze River Bridge.

The random variables of the suspension bridge were the elasticity modulus of the concrete, steel box girder, and cable; the cross-sectional areas of the main girder, pylon, and cable; the unit weights of steel and concrete; and the moving vehicle load. Statistical distributions of the above parameters are given in Table 1 and are based on the cable-stayed bridge in Lu et al. [24].

The upper and lower bound of the random variables were determined according to the  $3\sigma$  principle [30], where the range of the samples is defined as " $\mu \pm 3\sigma$ ". Due to that the wires have manufacturing errors and the number of wires is huge, in the present study, the coefficient of variation for cables and suspenders was assumed as 0.05.

**Table 1.** Statistical distributions of the random variables.

Items (unit)	Symbol	Distribution	Mean Value	Coefficient of Variation	Lower Bound	Upper Bound
Elasticity modules of concrete (MPa)	$E_1$	Lognormal distribution	$3.64 \times 10^4$	0.1	$2.548 \times 10^4$	$4.732 \times 10^4$
Elasticity modules of suspenders (MPa)	$E_2$	Lognormal distribution	$1.90 \times 10^5$	0.1	$1.33 \times 10^5$	$2.47 \times 10^5$
Cross-sectional area of girders ( $m^2$ )	$A_1$	Lognormal distribution	20.846	0.05	17.72	23.972
Cross-sectional area of individual parallel wire ( $m^2$ )	$A_2$	Lognormal distribution	$1.4 \times 10^{-4}$	0.05	$1.19 \times 10^{-4}$	$1.61 \times 10^{-4}$
Unit weight of concrete ( $kN.m^{-3}$ )	$\gamma_1$	Normal distribution	26.56	0.05	22.57	30.55
Unit weight of steel ( $kN.m^{-3}$ )	$\gamma_2$	Normal distribution	78.5	0.05	66.71	90.29

4.2. Traffic Load Modeling Using Weigh-in-Motion Data

Weigh-in-motion (WIM) data collected from a highway bridge in China were selected for the probabilistic modeling of traffic loads. The WIM system is illustrated in Figure 7, and more detailed information can be found in Lu et al. [11]. The traffic parameters utilized in the present study were vehicle weights, axle weights, driving lanes, and vehicle spacing. The proportion of trucks and the ratio of truck overloading were assumed as 12% and 21%, respectively.

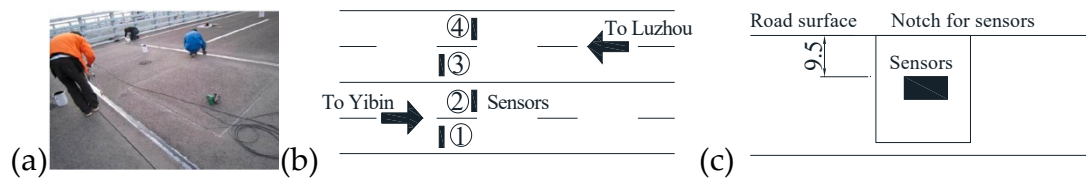


**Figure 7.** Weigh-in-motion system of a highway bridge: (a) site photos; (b) plane view; (c) elevation view unit: mm.

All vehicles were classified into six types, based on vehicle configurations and axle characteristics. The occupancy of the different vehicle types and their distributions in each lane are displayed in Figure 8.

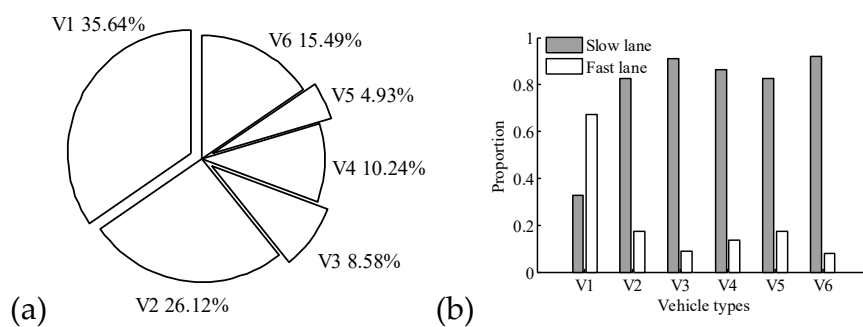


**Figure 8.** Proportion of vehicles (a) Vehicle types; (b) driving lanes.

As it can be seen in Figure 8a, light cars (V1) had the highest proportion of 35.64%, while two-axle (V2) and six-axle trucks (V6) had a higher proportion compared to other types of trucks. As it can be observed in Figure 8b, there is a high probability that the light cars are driving in the fast lane, while heavy trucks more mostly likely to drive in the slow lane. This phenomenon is in accordance with the practical situation.

The V6 trucks were selected as a prototype to investigate the probability of vehicle loads. Figure 9a shows histograms of the distribution of monitored empirical gross vehicle weights (GVWs). They were

fitted using a Gaussian mixture model (GMM) that is a combination of several Gaussian distributions. The two peaks of the PDF in Figure 9a represent the normal and overloaded trucks. It can be observed that the GVW followed a multimodal distribution, where the truck overloading effect was captured by the probabilistic model. Figure 9b plots the relationship between axle weight (AW) and GVW, where the star, circle, and plus symbols represent the weights of the first, second, and fifth axle, respectively, and  $AW_{ij}$  represents the AW of the  $j$ -th axle of the  $i$ -th type of vehicles. It is observed that the AW and GVW were almost linearly dependent.

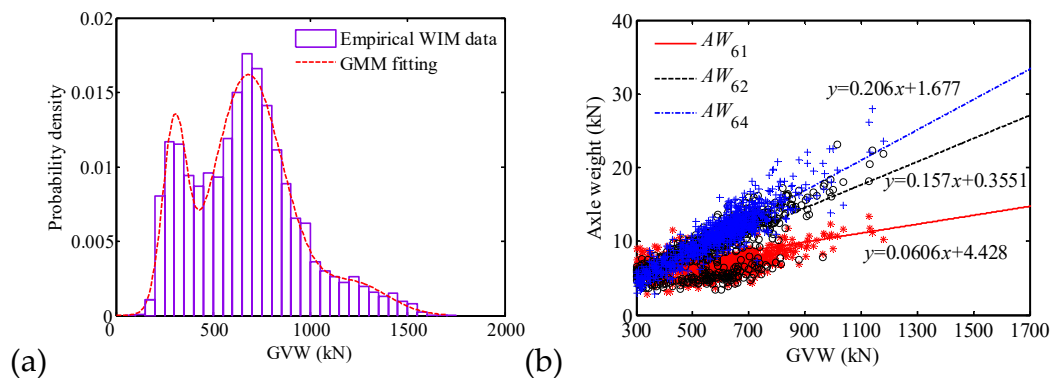


**Figure 9.** Probability distribution of V6 trucks: (a) PDF of GVWs; (b) relation between the GVW and the axle weight.

Based on the estimated probability distribution models, a stochastic traffic load model was developed using MCS. Figure 10 plots the simulated dense traffic flow model, where each vehicle was simulated as a label. The stochastic traffic load model contained the parameters of vehicle type, GVW, driving lane, and vehicle spacing.

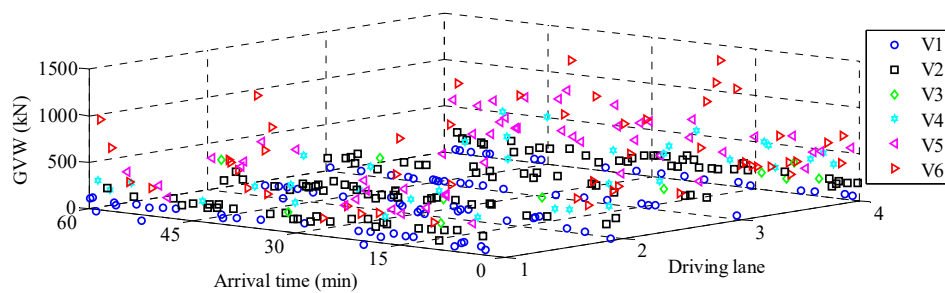


**Figure 10.** Stochastic load model for dense traffic flow.

#### 4.3. Reliability Analysis Based on the DBN Approach

Since structural failure is determined by the internal force of the bridge components, an appropriate FE model is essential to conduct the structural mechanical analysis. An FE of the bridge was developed in the commercial software ANSYS (Figure 11).

Girders and pylons were modeled with Beam188 elements, and the main cables and girders were modeled with Lin180 elements. The main cable and the pylon were connected with coupled degrees of freedom, while the bottom parts were fully constrained. The initial tension forces in the main cable and suspenders were introduced as pre-stressed tension.

Using the FE model, the structural response can be approximated through the DBN. Initially, 20 uniformly-distributed training samples were selected as the input data. Corresponding structural response including cable forces and bending moments, were computed using the FE model and were used as the output data. The DBN was treated following the framework presented in Figure 3. As an

example, the approximated cable force is presented in Figure 12. It can be observed that the response surface has captured the nonlinearity of structural mechanics.

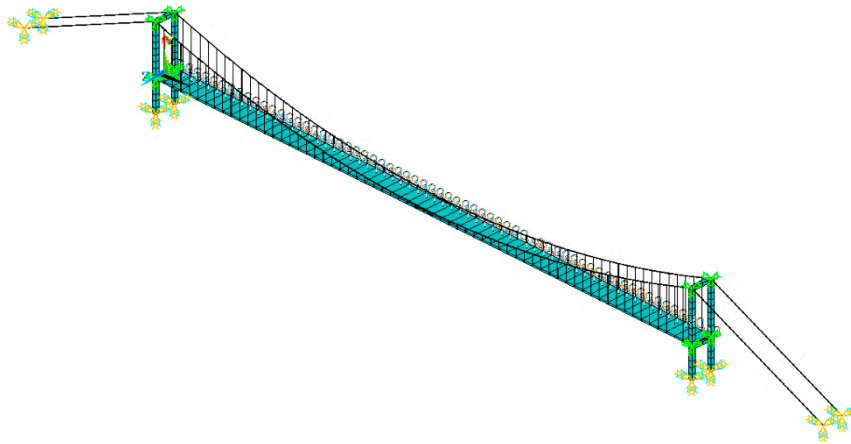


Figure 11. Finite element model in ANSYS of the suspension bridge.

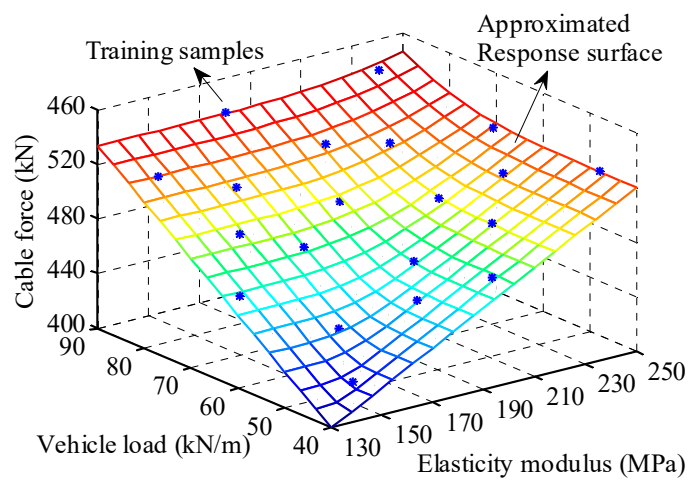


Figure 12. Simulated response surface and training samples of the cable force based on DBNs.

In general, there are three types of failure modes related to bridge components: suspender fracture, main cable rupture, and girder bending moment failure. The reliability index of each bridge component is shown in Figure 13.

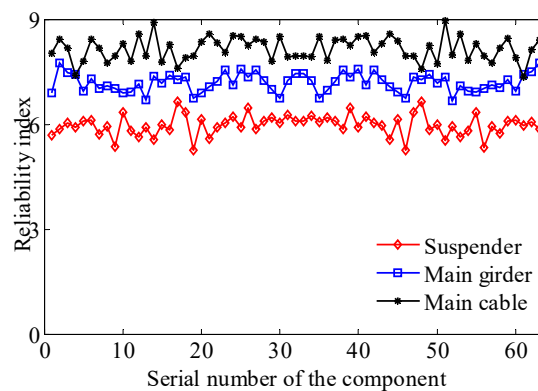


Figure 13. Reliability index of the bridge components.

It can be observed that the suspender had a relatively lower reliability index, while that of the main cable was the highest. Therefore, the first component more likely to fail should be the suspender. The most important step for the system reliability evaluation is to develop the fault tree of the structural system. The fault tree is composed of failure sequences, which can be evaluated based on the  $\beta$ -bound method.

#### 4.4. System Reliability Evaluation

According to the first failure searching procedure, the components that are likely to fail were H20 and H44. Since the failure mode of suspenders is brittle failure, the failed cable should be directly removed from the structural system. Subsequently, the structural system was updated and approximated by the DBNs. At the second stage, the components that were likely to fail were stiffening girders associated with G19, G21, G43, and G45. Since the failure mode of girders is plastic failure, a hinge should be added at the node between two girder elements. At the third failure stage, the main cable is the most likely to fail component associated with C18, C20, C22, C42, C44, and C46. Consequently, the three-level fault tree of the bridge structural system is constructed, as shown in Figure 14, where  $\beta_c$  is the conditional reliability index of the component corresponding to each failure stage.

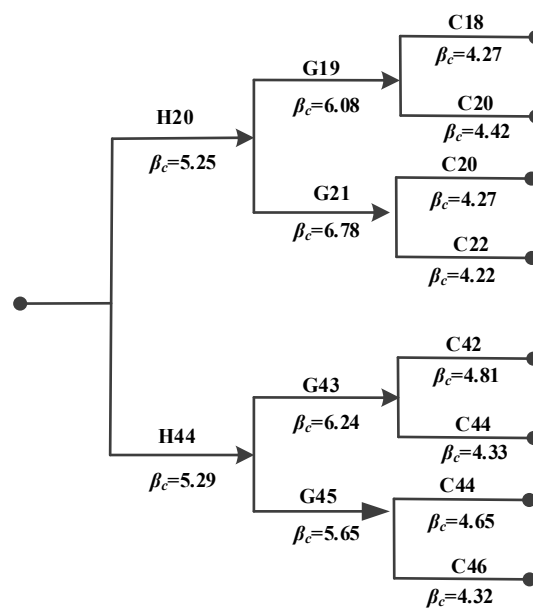


Figure 14. Fault tree of the suspension bridge.

Subsequently, the system reliability of the bridge was estimated through the series-parallel connection criterion. The corresponding series-parallel relationship is presented in Figure 15. It can be observed that the system reliability index was 9.63 by considering the three-level fault tree.

According to the standard for structural reliability of highway engineering in China, a bridge controlled by brittle failure should have a reliability index greater than 5.2. Therefore, the bridge used in the present study has an adequate safety factor during its lifetime. Nevertheless, fatigue-corrosion damage is the main factor that leads to of bridge safety degradation. In future studies, th cable strength should be determined and updated in the system reliability evaluation.

Cable damage due to the fatigue-corrosion effect is a critical factor that may lead to service life-shortening, safety threats, and increasing life-cycle cost. Thus, the effect of cable damage on the system reliability of suspension bridge deserves investigation. According to the cable strength degradation model shown in Figure 3, the system reliability of a bridge is adaptively updated. Figure 16

shows the degradation curve of the system reliability of the suspension bridge based on the service lifetime of the suspender.

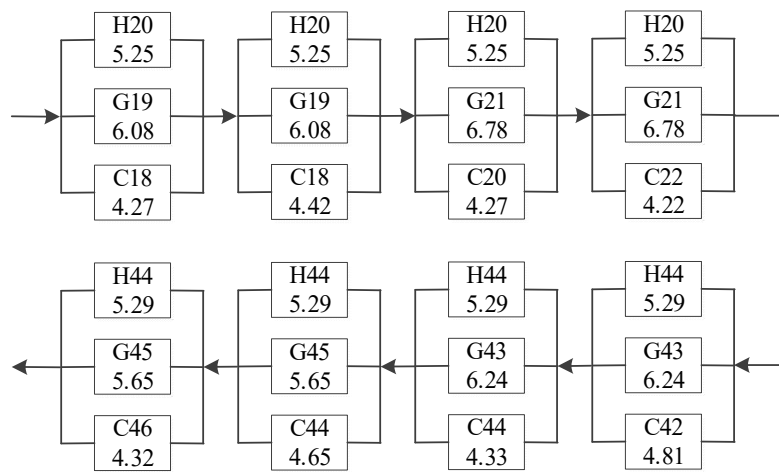


Figure 15. Series-parallel relationship of the three-level.

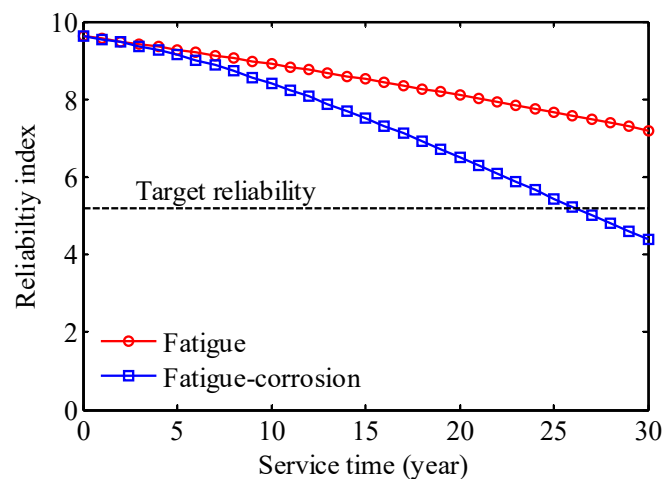


Figure 16. Influence of the cable strength degradation on the system reliability of the suspension bridge.

It can be observed that cable degradation due to fatigue damage leads to a slow reduction of the system reliability index from 9.63 to 7.22. However, the combined effect of fatigue-corrosion damage leads to a relatively sharp decrease of the system reliability index from 9.63 to 4.41. Therefore, cable corrosion is the dominant factor affecting bridge safety. In addition, given the target reliability index of 5.2, the suspension bridge has sufficient safety capacity accounting for cable fatigue damage. On the other hand, considering the fatigue-corrosion damage of suspenders, the maintenance time for cable replacement should be 26 years.

### 5. Conclusions

An intelligent approach for structural system reliability evaluation based on DBNs was presented. Mathematical models for system reliability evaluation of cable-stayed bridges were derived taking into consideration the structural nonlinearity and high-order statically indeterminate characteristics. The theoretical basis for utilizing DBNs to approximate the structural load was introduced. A computational framework was presented to illustrate the procedures followed to evaluate the bridge

system reliability via DBNs. The feasibility of the computational framework was demonstrated in a case study using a prototype suspension bridge. The conclusions are summarized as follows:

- (1) DBN provides an accurate approximation of the load effect of a cable-supported bridge, taking into consideration the structural nonlinearity in the behavior of the system. Thus, DBN can be utilized as a meta-model for a large number of simulations as a result of reliability analysis.
- (2) The suspender was found to have a relatively low reliability index, while that of the main cable was the highest. Therefore, the first component that was mostly likely to fail should be the suspender. In addition, the degradation of suspenders due to fatigue-corrosion damage was found to have a significant effect on the system reliability of the cable-supported bridge.
- (3) The system reliability index of the prototype suspension bridge is 9.63 considering the three-level system fault tree. Accounting for fatigue damage and fatigue-corrosion damage, the system reliability index decrease to 7.22 and 4.41, respectively.
- (4) According to the design standard for the structural reliability of highway bridges in China, a bridge controlled by brittle failure should have a reliability index greater than 5.2. Cable replacement should take place after 26 years of service time accounting for the fatigue-corrosion damage of suspenders.

Since fatigue-corrosion damage is the main factor leading to bridge safety degradation, further studies should focus on the cable degradation behavior and its effect on the failure sequence of bridges. In addition, more site-specific inspection data of the cables are needed to formulate the cable replacement scheme. Wind loads, seismic loads, and temperature loads should be taken into consideration in the reliability model, since these parameters are more critical for flexible bridges. Finally, structural health monitoring data can be employed to update the reliability model.

**Author Contributions:** Conceptualization, N.L.; Methodology, Y.L.; Data curation, X.X.; Writing—original draft preparation, N.L.; Writing—review and editing, N.L.; Supervision, M.N.; Project administration, N.L.; Funding acquisition, N.L. All authors have read and agreed to the published version of the manuscript.

**Funding:** This research was funded by [National Science Foundation of China] grant number [51908068], [National Science Foundation of Hunan Province] grant Numbers [2020JJ5140 and 2020JJ5589], [Open Fund of Key Laboratory of Bridge Engineering Safety Control in the Department of Education in Changsha University of Science and Technology] grant numbers [19KF03 and 19KB02], and [Innovation Platform Open Fund Project of Hunan Education Department] grant number [19K002]. The APC was funded by Changsha University of Science and Technology.

**Conflicts of Interest:** The authors declare no conflict of interest.

## References

1. Lu, N.; Beer, M.; Noori, M.; Liu, Y. Lifetime deflections of long-span bridges under dynamic and growing traffic loads. *J. Bridge Eng.* **2017**, *22*, 04017086. [[CrossRef](#)]
2. Sun, Z.; Zou, Z.; Zhang, Y. Utilization of structural health monitoring in long-span bridges: Case studies. *Struct. Control Health Monit.* **2017**, *24*, e1979. [[CrossRef](#)]
3. Sun, B.; Zhang, L.; Qin, Y.; Xiao, R. Economic performance of cable supported bridges. *Struct. Eng. Mech.* **2016**, *59*, 621–652. [[CrossRef](#)]
4. Shama, A.; Jones, M. Seismic Performance-Based Design of Cable-Supported Bridges: State of Practice in the United States. *J. Bridge Eng.* **2020**, *25*, 04020101. [[CrossRef](#)]
5. Larsen, A.; Larose, G. Dynamic wind effects on suspension and cable-stayed bridges. *J. Sound Vib.* **2015**, *334*, 2–28. [[CrossRef](#)]
6. Gong, X.; Agrawal, A. Safety of cable-supported bridges during fire hazards. *J. Bridge Eng.* **2016**, *21*, 04015082. [[CrossRef](#)]
7. Zhou, L.; Wang, X.; Ye, A. Shake table test on transverse steel damper seismic system for long span cable-stayed bridges. *Eng. Struct.* **2019**, *179*, 106–119. [[CrossRef](#)]
8. Xu, Y.; Øiseth, O.; Moan, T.; Naess, A. Prediction of long-term extreme load effects due to wave and wind actions for cable-supported bridges with floating pylons. *Eng. Struct.* **2018**, *172*, 321–333. [[CrossRef](#)]

9. Wang, F.; Xu, Y.L. Traffic load simulation for long-span suspension bridges. *J. Bridge Eng.* **2019**, *24*, 05019005. [[CrossRef](#)]
10. Jiang, C.; Wu, C.; Cai, C.S.; Jiang, X.; Xiong, W. Corrosion fatigue analysis of stay cables under combined loads of random traffic and wind. *Eng. Struct.* **2020**, *206*, 110153. [[CrossRef](#)]
11. Lu, N.; Ma, Y.; Liu, Y. Evaluating probabilistic traffic load effects on large bridges using long-term traffic monitoring data. *Sensors* **2019**, *19*, 5056. [[CrossRef](#)] [[PubMed](#)]
12. Mehrabi, A.; Ligozio, C.; Ciolko, A.; Wyatt, S. Evaluation, rehabilitation planning, and stay-cable replacement design for the hale boggs bridge in Luling, Louisiana. *J. Bridge Eng.* **2010**, *15*, 364–372. [[CrossRef](#)]
13. Jahangiri, V.; Yazdani, M. Seismic reliability and limit state risk evaluation of plain concrete arch bridges. *Struct. Infrastruct. Eng.* **2020**, 1–21. [[CrossRef](#)]
14. Lu, N.; Liu, Y.; Deng, Y. Fatigue reliability evaluation of orthotropic steel bridge decks based on site-specific weigh-in-motion measurements. *Int. J. Steel Struct.* **2019**, *19*, 181–192. [[CrossRef](#)]
15. Dai, H.; Zhang, B.; Wang, W. A multiwavelet support vector regression method for efficient reliability assessment. *Reliab. Eng. Syst. Saf.* **2015**, *136*, 132–139. [[CrossRef](#)]
16. Lu, N.; Liu, Y.; Beer, M. System reliability evaluation of in-service cable-stayed bridges subjected to cable degradation. *Struct. Infrastruct. Eng.* **2018**, *14*, 1486–1498. [[CrossRef](#)]
17. Cui, T.; Li, S. Deep learning of system reliability under multi-factor influence based on space fault tree. *Neural Comput. Appl.* **2019**, *31*, 4761–4776. [[CrossRef](#)]
18. Wang, H.; Wang, G.; Li, G.; Peng, J.; Liu, Y. Deep belief network based deterministic and probabilistic wind speed forecasting approach. *Appl. Energy* **2016**, *182*, 80–93. [[CrossRef](#)]
19. Lu, N.; Noori, M.; Liu, Y. Fatigue reliability assessment of welded steel bridge decks under stochastic truck loads via machine learning. *J. Bridge Eng.* **2017**, *22*, 04016105.3. [[CrossRef](#)]
20. Bao, Y.; Tang, Z.; Li, H.; Zhang, Y. Computer vision and deep learning-based data anomaly detection method for structural health monitoring. *Struct. Health Monit.* **2019**, *18*, 401–421. [[CrossRef](#)]
21. Fink, O.; Zio, E.; Weidmann, U. Predicting component reliability and level of degradation with complex-valued neural networks. *Reliab. Eng. Syst. Saf.* **2014**, *121*, 198–206. [[CrossRef](#)]
22. Lee, Y.; Song, J. Finite-element-based system reliability analysis of fatigue-induced sequential failures. *Reliab. Eng. Syst. Saf.* **2012**, *108*, 131–141. [[CrossRef](#)]
23. Kang, W.; Song, J.; Gardoni, P. Matrix-based system reliability method and applications to bridge networks. *Reliab. Eng. Syst. Saf.* **2008**, *93*, 1584–1593. [[CrossRef](#)]
24. Liu, Y.; Lu, N.; Yin, X.; Noori, M. An adaptive support vector regression method for structural system reliability assessment and its application to a cable-stayed bridge. *Proc. Inst. Mech. Eng. Part O J. Risk Reliab.* **2016**, *230*, 204–219. [[CrossRef](#)]
25. Ma, Y.; Peng, A.; Su, X.; Wang, L.; Zhang, J. Modelling constitutive relationship of steel bar removed from corroded PC beams after fatigue considering spatial location effect. *ASCE J. Mater. Civil Eng.* **2020**. [[CrossRef](#)]
26. Ma, Y.; Guo, Z.; Wang, L.; Zhang, J. Probabilistic life prediction for reinforced concrete structures subjected to seasonal corrosion-fatigue damage. *ASCE J. Struct. Eng.* **2020**, *146*, 04020117. [[CrossRef](#)]
27. Faber, M.; Engelund, S.; Rackwitz, R. Aspects of parallel wire cable reliability. *Struct. Saf.* **2003**, *25*, 201–225. [[CrossRef](#)]
28. Li, H.; Lan, C.; Ju, Y.; Li, D. Experimental and numerical study of the fatigue properties of corroded parallel wire cables. *J. Bridge Eng.* **2012**, *17*, 211–220. [[CrossRef](#)]
29. Lin, K.; Pai, P.; Ting, Y. Deep belief networks with genetic algorithms in forecasting wind speed. *IEEE Access* **2019**, *7*, 99244–99253. [[CrossRef](#)]
30. Kamran, A.; Guozhu, L.; Rafique, A.F.; Zeeshan, Q.  $\pm 3$ -Sigma based design optimization of 3D Finocyl grain. *Aerosp. Sci. Technol.* **2013**, *26*, 29–37. [[CrossRef](#)]

**Publisher's Note:** MDPI stays neutral with regard to jurisdictional claims in published maps and institutional affiliations.



© 2020 by the authors. Licensee MDPI, Basel, Switzerland. This article is an open access article distributed under the terms and conditions of the Creative Commons Attribution (CC BY) license (<http://creativecommons.org/licenses/by/4.0/>).